LWT - Food Science and Technology 238 (2025) 118894

Contents lists available at ScienceDirect

LWT

journal homepage: www.elsevier.com/locate/lwt

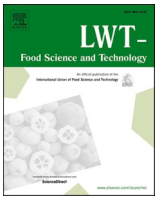

Evaluation of 3D printing inks and printed edible spoons made from food processing side streams

Marta Stachnik [a,b,*], Eija Kulju [c], Oskar Laaksonen [b]

[a] Nutrition and Food Research Center (NuFo), 20014, University of Turku, Finland
[b] Food Sciences, Department of Life Technologies, University of Turku, 20014, Turun Yliopisto, Turku, Finland
[c] Engineering, Chemical Engineering and Common Studies, 20520, Turku University of Applied Sciences, Finland

ARTICLE INFO

Keywords:
3D printing
Circular economy
Edible spoons
Side streams
Rheology

ABSTRACT

3D printing technology was used to develop prototypes of edible spoons from side streams of food and beverage production. All ink formulations were based on brewer's spent grain and supplemented with one of the following: apple or berry pulp, or powdered seeds from black currant or sea buckthorn. The printability of the food ink was assessed through rheological measurements, while the spoons were tested for their water and oil absorption, and water solubility and sensory quality. Inks exhibited elastic behavior at rest, becoming viscous under shear (phase shift angle from 14° to 80°). Both storage (G′) and loss (G″) moduli showed significant recipe-dependent variations. The recovery rate was notably low which was further reflected in the sagging of the ink after the print. All spoons nearly doubled their weight when submerged in water, but not in oil – on average 20 % increase in weight. Spoons made only with spent grain had significantly higher water solubility than other recipes. Spoons made with addition of berry pulp received the highest ratings, on average 6 out of 9 in hedonic scale; while other spoons were rated on average 5 out 9. When used to consume yogurt, the spoons did not alter its flavor. The texture of all spoons was considered appealing, with the 3D printing layers being either imperceptible or pleasant.

1. Introduction

The Food 2030 initiative, launched by the EU in 2016, aims to secure a sustainable and resilient food future. It addresses major challenges such as climate change, environmental degradation, and the increasing demand for sustainable food by promoting reduced food waste, repurposing of residues, and the efficient use of resources through collaboration and innovation (Food2023, 2025). Within this vision, a Circular Economy (CE) promotes the reuse, recycling, recovery, and reprocessing of both edible and inedible food components (FIT4FOOD2030, n.d.; Lugo et al., 2022). Processing of agricultural raw materials generates large, concentrated side streams, and their scale alone makes their management nontrivial (Caponio et al., 2022). For example, global apple processing produces several million tonnes of apple pomace per year; from an annual production of 366 million tonnes of apples, an estimated 3–4.2 million tonnes become pomace and related residual material (Bortolini et al., 2020). Wine production yields grape pomace (skins, seeds, stems) that is similarly generated at industrial scale and is known to contain phenolics such as stilbenes and resveratrol, as well as oil fractions with bioactive potential (Costa et al., 2019; Kaur et al., 2009; Matharu et al., 2016). Beer brewing produces particularly high volumes of by-products: brewer's spent grain (BSG), hot trub, and surplus yeast, with BSG alone reaching ~39 million tonnes annually worldwide and ~3.4 million tonnes in Europe (Mussatto & Roberto, 2008; Olajire, 2020; Osei et al., 2025; Singh & Saini, 2012). These streams are compositionally valuable — apple pomace is rich in polyphenols (e.g. epicatechin, catechin, quercetin) and pectin, a gelling and fermentable polysaccharide (Campos et al., 2020; Park et al., 2022); grape residues contain fibre and antimicrobial phenolics; spent grain is rich in insoluble fibre, protein, vitamins, and minerals (Costa et al., 2019). However, despite this biochemical value, most of these materials remain underutilised at scale and must be removed from production sites as wet, bulky biomass (Costa et al., 2019). Because these side-streams are generated in large quantities and have very high moisture content and organic load (often 70–80 % water in the case of brewery grain residues (Eche et al., 2025), they are heavy to transport, spoil rapidly, and require immediate removal from production sites (Fernandes & Silva, 2025). This increases handling and transport costs

* Corresponding author. Nutrition and Food Research Center (NuFo), 20014, University of Turku, Finland.
E-mail address: marta.m.stachnik@utu.fi (M. Stachnik).

https://doi.org/10.1016/j.lwt.2025.118894
Received 27 June 2025; Received in revised form 24 November 2025; Accepted 8 December 2025
Available online 11 December 2025

and, if they are landfilled or otherwise discarded as untreated wet biomass, leads to odour, leachate formation, and anaerobic degradation that produces methane-rich greenhouse gas emissions. In this sense, sidestreams represent both a nutrient-rich resource and an environmental liability if not repurposed (Chickering et al., 2023).

Single-use plastic cutlery has faced global bans due to its environmental impact (Ha, 2023). Edible cutlery, typically made from sorghum, rice, or millet flours, presents a sustainable alternative. It is durable, biodegradable, heat-resistant, and offers nutritional value and improved dining experiences (Natarajan et al., 2019; Roy & Morya, 2022). BSG has gained attention as a promising ingredient in edible packaging (Oztuna Taner et al., 2023; Shroti & Saini, 2022) and tableware (Nehra et al., 2024). Other innovations include soy protein–based spoons enhanced with morning glory fiber (Choeybundit et al., 2022), spoons combining mosambi peel and sago (Siddiqui et al., 2022), edible bowls made from ragi, wheat, and rice flours (Rishi et al., 2024), or edible straws from various flours (Yavagal et al., 2020). Commercial edible cutlery options are increasingly available (Koovee, incrEDIBLE Eats, Bakeys, and EdiblePRO).

Additive manufacturing, or 3D printing, is particularly attractive in food applications because it can produce complex, customized geometries without the need for dedicated molds (Aimar et al., 2019). Instead of fabricating a new mold for every design change, the shape can be altered digitally and printed directly, which makes iteration and personalization fast and low-cost (Lipton et al., 2010; Pulatsu & Lin, 2021). **Understanding properties of food inks is essential for successful 3D printing, as these characteristics directly impact print quality and structural integrity. Critical factors include rheological behavior (such as viscosity, recovery index shear thinning behavior and flowability), structural stability, and physio-chemical properties like gelation and melting point** (Mantihal et al., 2017)**. In addition, printing parameters—such as extrusion speed, nozzle size, and movement rate play a significant role in determining the quality of the final product** (Feng et al., 2018)**.**

The objective of this research was to create edible spoon prototypes through the application of 3D printing technology. These prototypes were fabricated using a novel food-grade ink derived from by-products generated during beer, cider and wine production, and seed oil extraction. Inks printability was assed via rheological measurements and spoons were tested for their water and oil absorption and sensory attributes.

2. Materials and methods

2.1. Materials

The base food ink is made from brewer's spent grain (22 %, Kupittaa Campus Brewery, Turku AMK, Finland), oat flour (22 %), wheat flour (33 %) and one of the following side streams (22 %): three types of defatted berry and seed cakes from commercial berry oil extraction (Aromtech Oy, Tornio, Finland): black currant seeds, sea buckthorn berries and seeds; apple pulp from cider production (Brinkhall Sparkling Oy, Halikko, Finalnd) and berry pulp from wine production (Teiskon Viini, Kämmenniemi, Finland). Berry cakes were first milled and then sifted with a sieve. Apple pulp and berries were homogenized using an immersion blender, after which, solid fragments (peel and seeds) were removed through screening. Fresh BSG was dried at around 85 °C for 2–3 h to 5 % moisture (Thai et al., 2022). BSG was then milled in a malt mill and sifted via a sieve. Oat flour was selected based on its health advantages (Paudel et al., 2021). Wheat was included due to gluten's capability to create a protein network and work as a binder (Fahmy et al., 2021).

2.2. Sample preparations

Food inks of the appropriate consistency for printing was developed through an iterative process; the target criterion was that all inks could still be extruded using the same printing settings. Ink containing wheat, oat and BSG flours was considered as a control sample, base ink. Addition of other side streams following variations of the ink's formulations.

- wheat, oat, brewers spent grain – base ink, BSG;
- wheat, oat, brewers spent grain, berry pulp – BR;
- wheat, oat, brewers spent grain, defatted black currant seeds – MS;
- wheat, oat, brewers spent grain, defatted sea buckthorn berries – TM
- wheat, oat, brewers spent grain, defatted sea buckthorn seeds – TS;
- wheat, oat, brewers spent grain, apple pulp from cider production – AP.

Appropriate amounts of each flour were weighed and mixed. Water was then added to reach a total moisture content of 85 %. For samples containing apple or berries, the amount of added water was reduced to account for the moisture contributed by the fruit pulp. The dough was mixed for 15 min, transferred into the syringe cartridge, and allowed to rest for 30 min before printing.

2.3. Methods

2.3.1. Rheological analysis

Tests were conducted at 20 °C after pre-shear (0.5 Pa for 60 s) and rest phase (90 s). Amplitude sweeps were performed over a strain range of 0.001–1000 % at 1 Hz, and frequency sweeps at a constant strain of 0.01 % across 0.1–50 Hz. The creep-recovery test applied a constant stress of 1 Pa for 480 s, followed by a recovery phase at 0 Pa for the same duration. To minimize slippage and improve measurement reliability, serrated parallel plates (20 mm diameter) with a 1 mm gap were used. Tests were performed on a freshly made inks, separate from printing tests. Based on creep-recovery data recovery parameter – R (%) was calculated as the ratio of final (J_min) and maximum (J_max) compliance (Tarancón et al., 2015):

$$R(\%) = \frac{J_{max} - J_{min}}{J_{max}} \cdot 100. \quad (1)$$

2.3.2. 3D printing

Food ink formulations were printed using a Brinter ONE Multitool 3D Bioprinter (Winston-Salem, NC) with extrusion-based technology. The ink, stored in 10 mL containers, was extruded onto baking paper following a spoon-shaped pattern (Fig. 3a) designed in AutoCAD (Autodesk Inc., San Francisco, CA) and sliced using the printer's software (Fig. 3b). Printing was carried out at room temperature of 21 °C at 400 mbar pressure and 7 mm/s extrusion speed using a 0.84 mm metal nozzle. Spoons were baked at 130 °C for 30 min.

Assessment of an ink's printability is primarily based on its rheological properties. Many authors have reviewed the rheological ranges associated with good printability in extrusion-based food printing (Godoi et al., 2016; Hussain et al., 2021; Oh et al., 2024). As food materials exhibit a wide variety of rheological behaviours, the optimal parameter ranges are material-specific. According to the literature, dough formulations should be considered printable when they exhibit elastic-dominant behaviour ($G' > G''$; where $G' \approx 10^3$–10^4 Pa), tan $\delta \approx$ 0.14–0.17, and a phase angle $\delta < \sim 35°$, corresponding to solid-like viscoelasticity that enables self-support after extrusion (Čukelj Mustač et al., 2023). Shape fidelity was defined as ≤ 10 % deviation of measured dimensions (width, height, thickness) (L. Zhang et al., 2018).

2.3.3. Physiochemical properties of the spoons

Water absorption was measured following ASTM D570 methodology (Choeybundit et al., 2022): spoons were dried at 50 °C for 24 h, then

immersed in 250 ml of distilled water for another 24 h. Excess water was drained and blotted with absorbent paper. Water absorption was calculated as:

$$\text{Water absorption } (\%) = \frac{M_1 - M_0}{M_0} \cdot 100\%, \quad (2)$$

where M_0: initial weight and M_1: post-water absorption weight of the spoons [g].

Following the same author (Choeybundit et al., 2022), water solubility was determined by immersing 3 g of sample in 30 ml of distilled water and mixing on a rotary shaker (120 rpm, 25 °C) for 24 h. The residue was then filtered, dried at 105 °C for 24 h, and weighed. Solubility was calculated as:

$$\text{Solubility } (\%) = \frac{M_1 - M_0}{M_0} \cdot 100\%, \quad (3)$$

where M_0: initial weight of the filter paper and M_1: weight of the filter paper and the collected sediment [g].

Swelling was assessed by comparing spoon dimensions before and after 24 h of water immersion, following (Gamero et al., 2019):

$$\text{Degree of swelling } (\%) = \frac{D_1 - D_0}{D_0} \cdot 100\%, \quad (4)$$

where D_0: initial dimension and D_1: final dimension [mm].

Oil absorption was measured according to (Nehra et al., 2024): whole spoons were submerged in 20 ml of sunflower oil for 1 h. Absorption was calculated as:

$$\text{Oil absorption } (\%) = \frac{M_1 - M_0}{M_0} \cdot 100\%, \quad (5)$$

where M_0: initial weight of the spoon and M_1: weight of the spoon after submersion [g].

2.3.4. Sensory evaluation

The sensory evaluation of the edible spoons and their influence on food perception was conducted using a structured questionnaire with 12 panelists (mostly female, aged 24–32, with two older participants, a mix of students and staff from the Food Sciences unit at the University of Turku with previous experience in conducting sensory evaluations). An ethics approval was obtained from university committee of Human Sciences, Humanities and Social Sciences Division, University of Turku, Finland (TY/136/06.January 01, 2024, obtained February 12, 2024). Participants provided their consent at the time of the study. Participation was voluntary with no monetary compensation. Nine-point hedonic scales (Sood & Deepshika, 2018) were used to assess the spoons' color, aroma, attractiveness, texture, and taste, as well as any impact on the smell of a selected food—lactose-free yogurt, chosen for its neutral flavor and broad appeal.

Each panelist received a tray with randomized, coded with three-digit numbers edible spoons in the first row. The middle section included a bowl of yogurt, a spit cup, and a white plate for contrast. The last row contained a glass of water and unblinded reference spoons (plastic, biocomposite, wood, and metal), arranged to match the question order. Participants first rated spoon appearance, smell and texture under fingers. They then consumed yogurt with coded spoons, evaluating mouthfeel, texture, and whether 3D printing layers were noticeable or pleasant. Next, they ranked all spoons (including reference spoons) from most to least preferred for consumption. Finally, they tasted a clean part of each edible spoon, rated its flavor (0–9). Survey preparation and data collection was done using Compusense20 (Compusense Inc., Guelph, Ontario, Canada) software. Answers were collected anonymously.

2.3.5. Statistical analysis

Measurements were done in triplicates. Statistical analysis was performed in IBM SPSS Statistics 27. ANOVA with Tukey's HSD was used for recipe comparisons. Paired t-tests assessed changes in spoon dimensions before and after water or oil submersion. Significance was set at $p < 0.05$.

3. Results

3.1. Rheological assessment of ink's printability

For all tested recipes, the storage modulus (G') was consistently higher, indicating a predominant elastic nature in the inks (Fig. 1a). Among the samples, the berry pulp ink (BR) exhibited the highest moduli within the LVR ($G' = 30{,}512$ Pa; $G'' = 7502$ Pa), while the blackcurrant seed flour ink (MS) showed the lowest ($G' = 13{,}604$ Pa; $G'' = 3481$ Pa). The BR recipe had the highest yield stress ($\tau = 2062.4$ Pa), and TS the lowest ($\tau = 277.6$ Pa). At 0.001 % strain, phase shift angles ranged from 9° to 19°, with AP being the most elastic (9.3°) and BR the least (18.9°). At 1000 % strain, phase shift angles ranged from 76.1° (TS) to 80.3° (AP), indicating a predominantly viscous response.

In the frequency sweep, G' showed a stronger frequency dependence than G'', increasing from ~11,000 Pa to 31,000–51,000 Pa, while G'' increased from ~6000 Pa to ~11,000 Pa (Fig. 1c). The highest moduli were observed in BR and BSG, and the lowest in MS and AP. Complex viscosity ($|\eta^*|$) decreased with increasing frequency (Fig. 1d), indicating shear-thinning behavior. This aligns with Graessley's entanglement theory (J.-P. Zhang et al., 2024), where higher frequencies disrupt hydrophobic interactions and reduce polymer entanglement density, weakening structural integrity.

The loss tangent (tan δ), defined as the ratio of G'' to G', provides insight into viscoelastic behavior. Values below 1 indicate solid-like characteristics, while values above 1 suggest liquid-like behavior. All samples exhibited tan $\delta < 0.35$, confirming their solid-like nature. The AP ink was the most elastic (tan $\delta = 0.20$), and BSG the least (tan $\delta = 0.35$). Yield stress (τ) values also varied significantly between formulations, with FR showing the highest (2062 Pa) and TS the lowest (278 Pa), reflecting differences in structural integrity. A sufficiently high yield point is crucial for 3D printing, as it prevents material sagging and supports precise extrusion (Liu et al., 2020). ANOVA confirmed significant differences in G', G'', and τ values ($p < 0.05$), indicating that formulation composition strongly influences rheological behavior (Table 1).

The creep-recovery test assesses an ink's deformation under load (printing) and its structural recovery post-load (post-printing). High compliance indicates easy deformation, while low compliance reflects rigidity (Menard & Menard, 2020). MS and TS inks, with the lowest G' values (Fig. 1b), showed the highest deformation during creep. In contrast, BSG exhibited the lowest strain, followed by AP and BR—samples with the highest elastic moduli. None of the inks fully recovered after unloading, indicating predominantly viscoelastic fluid behavior. As the creep-recovery curves are typically nonlinear and complex, the percentage of recovery (R) is used as a simplified descriptor. The highest R value was observed for BR ink (35.4 %), followed by AP (25.8 %) and TM (20.1 %), whereas the lowest recovery was seen in TS (7.4 %) and MS (8.6 %). These results indicate that BR and AP inks possess stronger internal structures and better elastic recovery, suggesting superior shape retention after printing. Conversely, the poor recovery of TS and MS reflects a higher degree of irreversible deformation, which may compromise print fidelity. Based on the analysis of compliance curves and R indices, all six inks can be classified as viscoelastic liquids, with statistically significant differences between recipes.

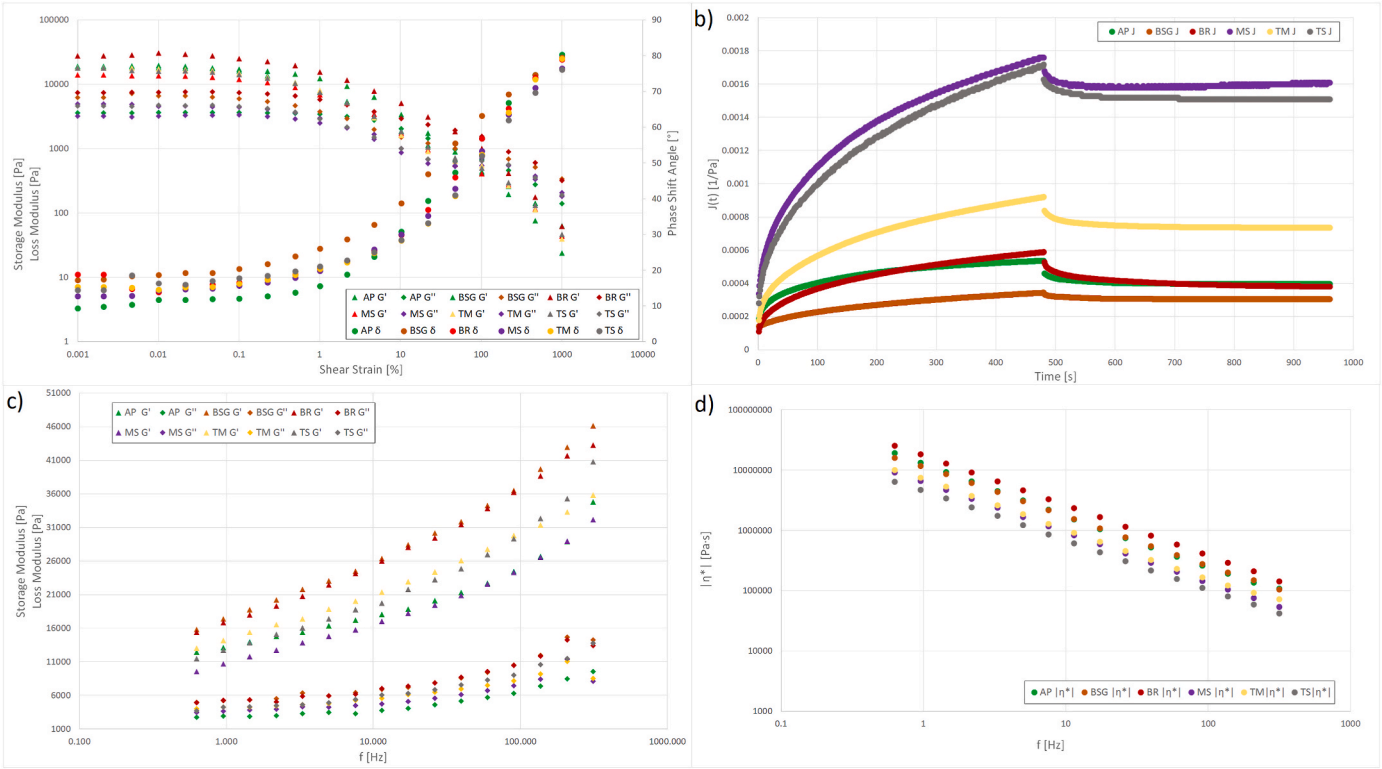

Fig. 1. Inks' printability assessment a) amplitude sweep test – changes in storage G′ and loss moduli G″, and phase shift angle δ as a function of shear strain; b) creep-recovery test as creep compliance curve c) frequency sweep test - storage and loss moduli as a function of frequency; d) frequency sweep test - complex viscosity as a function of frequency.

Table 1
Selected rheological properties of inks.

Samples	G' [Pa]	G'' [Pa]	τ [Pa]	δ [°] at γ = 0.001 %	δ [°] at γ = 1000 %	tanδ [−] in LVR	R%
AP	18 152c (SD = 220.40)	3841.7c (SD = 70.07)	691.18a (SD = 4.72)	9.33 (SD = 0.69)	80.34 (SD = 1.50)	0.20a (SD = 0.013)	25.8a
BSG	19 441c (SD = 249.98)	6606.5a (SD = 304.36)	577.12b (SD = 7.64)	18.30 (SD = 0.76)	79.52 (SD = 2.23)	0.35b (SD = 0.015)	11.0c
BR	30 512a (SD = 995.60)	7 502a (SD = 181.18)	2062.40c (SD = 19.53)	18.87 (SD = 0.74)	79.00 (SD = 2.19)	0.26cd (SD = 0.014)	35.4b
MS	13 604d (SD = 136.15)	3481.5d (SD = 178.87)	366.73d (SD = 2.92)	12.75 (SD = 0.80)	76.44 (SD = 2.20)	0.25de (SD = 0.014)	8.6d
TM	17 515c (SD = 368.13)	4548.2b (SD = 123.61)	397.45e (SD = 2.66)	15.32 (SD = 0.29)	79.21 (SD = 2.59)	0.27de (SD = 0.006)	20.1e
TS	16 038bc (SD = 135.33)	4 711b (SD = 384.13)	277.55f (SD = 6.49)	14.37 (SD = 1.14)	76.10 (SD = 3.12)	0.31e (SD = 0.022)	7.4f

LVR – linear viscoelastic region, defined as the strain range where G′ and G″ remain constant and parallel to the x-axis in log–log scale.
Means with different letters are significantly different ($p < 0.05$, Tukey's HSD).

3.2. 3D-printed spoons

Despite being printed with identical settings, the spoons exhibited noticeable shape variations (Fig. 2d), attributable to differences in rheological properties across the inks. In the AP spoons, a consistent breakage point was observed between the scoop and the handle. Interestingly, this occurred despite AP exhibiting relatively favorable rheological properties: the highest yield stress (τ = 691.2 Pa) and the second-highest recovery percentage (R% = 25.8 %). This suggests that failure may not stem from flow instability but rather from fiber embrittlement during drying. The apple pulp fibers likely shrank or fractured as water was removed, compromising structural integrity at the joint. This failure mode was not observed in spoons made from other materials.

The BR spoon demonstrated the most visible printed pattern, particularly on the handle. This correlates well with its rheological profile: the highest yield stress (τ = 2062 Pa), the highest recovery percentage (R% = 35.4 %), and the highest elastic modulus (G′ = 30,512 Pa). These values indicate a highly structured, elastic material that resisted deformation under stress and maintained the extruded shape, resulting in precise filament layering. Conversely, the TS spoon showed the least visible layering, which matched its status as the sample with the lowest τ (277.6 Pa), lowest R% (7.4 %), and one of the lowest G′ values (16,038 Pa). MS and TM spoons showed intermediate filament pattern visibility, aligning with their moderate rheological performance.

A common observation across all samples was poor filament recovery immediately post-extrusion (2c). Filaments flattened instead of maintaining their round profile, though this occasionally aided adhesion between infill and perimeter lines. A 0.84 mm nozzle was used to mitigate clogging, but this change introduced filament gaps—especially in curved regions of the handles. The issue was most prominent in spoons made with berry pulps, which also displayed the most distinct filament patterns. In contrast, spoons containing sea buckthorn flour had less visible surface features. Dimensional measurements further reflected material differences. The flattest spoons were from BR inks (min. thickness: 2.96 mm), while BSG produced the thickest (3.63 mm). MS and TM spoons had the narrowest handles (7.51 mm and 7.55 mm), whereas TS spoons were the widest at 9.46 mm. By comparison, the CAD design specified a target thickness of 4 mm and handle width of 10 mm (Fig. 2a). In addition to shape and texture, color variation was also observed and correlated with formulation. BSG spoons were the lightest, while BR, MS, and TS variants appeared visibly darker—likely due to ingredient composition and bake-induced browning. Especially spoons

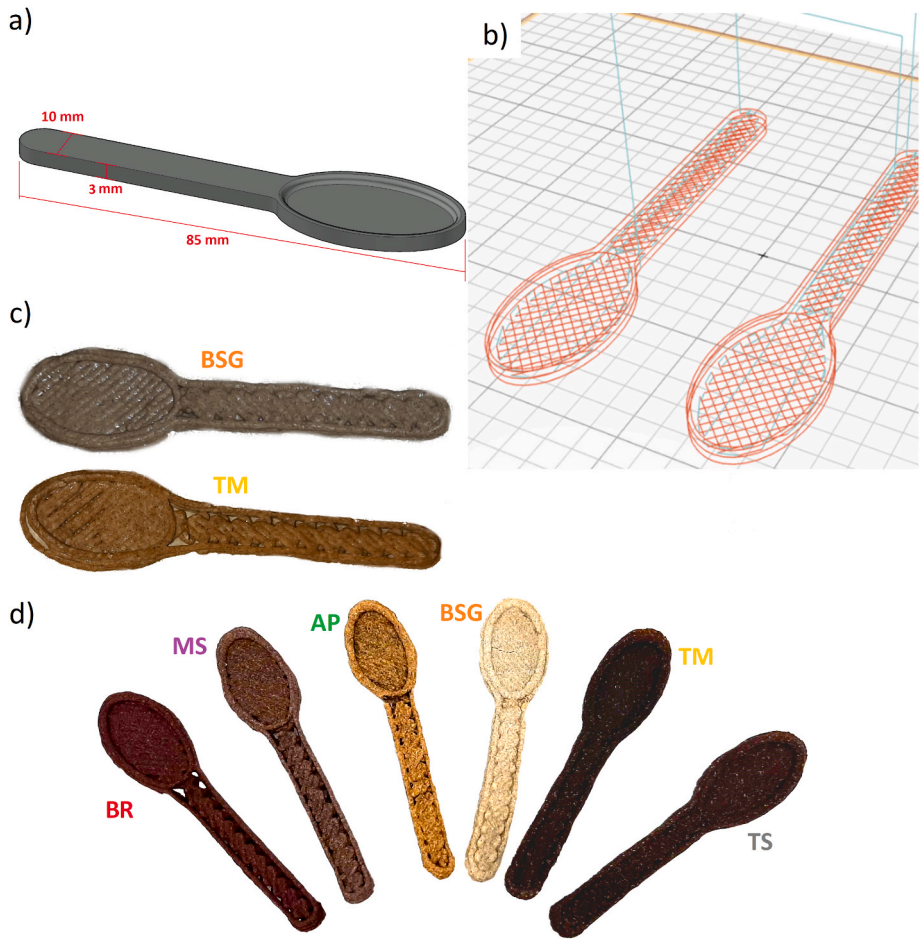

Fig. 2. The design of the edible spoon: a) Computer Aided Design (CAD) of the spoon; b) sliced geometry for 3D printer: 4 layers with 100 % infill and 45° filament orientation; c) spoons after printing, before baking; d) front view of spoons after baking.

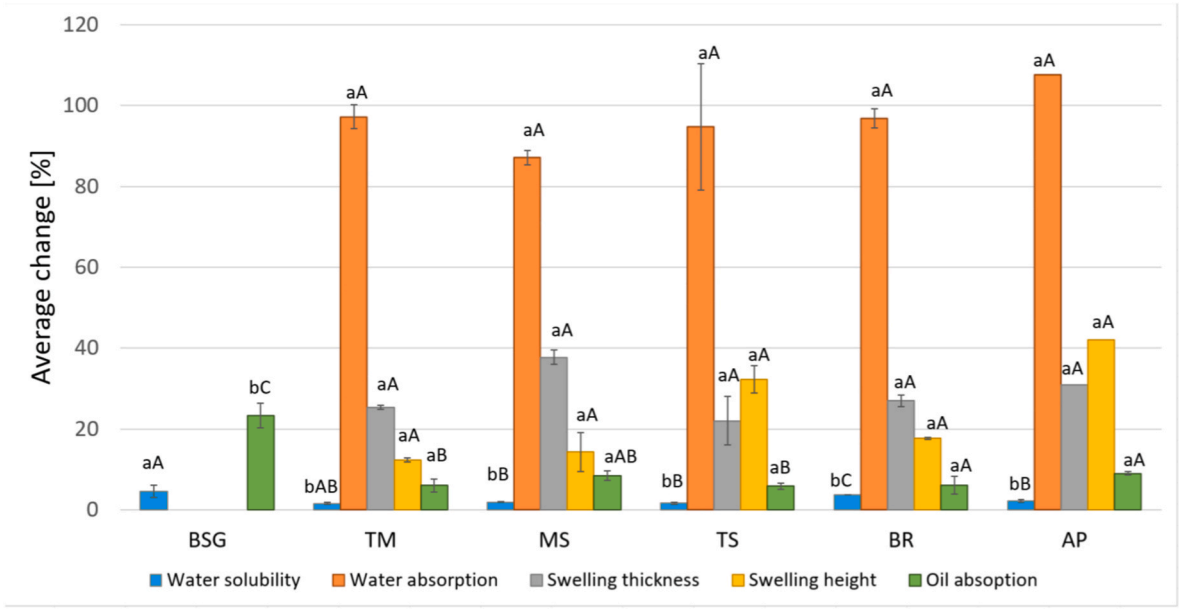

Fig. 3. Average percentage changes in physicochemical properties of 3D-printed spoons before and after treatment. Paired t-tests ($p < 0.05$) were used to assess whether each formulation exhibited a statistically significant change after treatment; significant within-formulation differences are indicated by lowercase letters. One-way ANOVA with Tukey's HSD post hoc tests ($p < 0.05$) were used to compare the percentage changes between different formulations; significantly different formulation groups are marked with capital letters. Bars that share a letter (either lowercase or uppercase) are not significantly different within their respective comparison type.

containing sea buckthorn residue darkened after baking.

3.3. Physiochemical analysis of the spoons

The quality of the spoon was assessed based on its water and oil absorption capacities, water swelling, and solubility (Fig. 3). These properties define how the spoons will interact with the food. The functional properties of six edible spoon formulations were assessed after soaking, with results presented as average percentage changes (Fig. 3). Water absorption was the dominant transformation across all formulations except for the BSG-based spoons, which disintegrated during soaking and therefore could not be evaluated for most parameters. Nevertheless, BSG exhibited the highest oil absorption (23.4 %) and the greatest water solubility (4.6 %), both significantly different from the other materials ($p < 0.05$). In contrast, the TM formulation demonstrated the most stable performance overall. It absorbed water up to 97.2 % of its final mass, with the lowest swelling in thickness (12.3 %) and low swelling in width, as well as minimal oil uptake and solubility. MS spoons absorbed less water (87.2 %) and exhibited the greatest width swelling (37.7 %), which was significantly higher than that of TM ($p < 0.05$). The AP-based spoons showed the highest water absorption (107.7 %) and the most pronounced swelling in thickness (42.0 %), coupled with moderately high oil absorption (9.0 %). Despite these differences in swelling and oil uptake, statistical analysis revealed no significant differences in water absorption among TM, MS, TS, BR, and AP. The only parameter with statistically significant variation beyond BSG was swelling width, particularly between MS and TM. Among tested spoons, the TM formulation demonstrated the highest structural resilience, whereas the BSG and AP formulations were the most prone to degradation and deformation.

3.4. Sensory evaluation of the spoons

The spoons made from berry pulp, BR, received the highest ratings across most categories, with the exception of mouthfeel texture, where the TM spoon was rated higher (Table 2). The majority of the lowest ratings were attributed to the TM spoon. Significant differences in ratings were observed for appearance, smell, color, shape, and overall attractiveness. Yet, the average scores were mostly around 5 out of 9, with the color and attractiveness of the BR spoon achieving higher scores of 7 out of 9. **In the final part of the study, panelists consumed yogurt using both edible and conventional reference spoons, and then ranked them from most to least pleasant (Fig. 4).** The metal spoon was the favorite—**67 % of participants ranked it first**. The **biocomposite spoon received 25 % of first-place votes**, while **33 % placed it second**, suggesting generally positive reception. Edible spoons received a wide distribution of rankings across positions 3 to 7, **indicating diverse personal preferences and no clear standout** among them. In contrast, the **wooden spoon was consistently disliked**, with **75 % of participants ranking it last**.

Table 2
Mean values of sensory evaluation by the panel (n = 12) of edible spoons on the hedonic scale (0 - very unpleasant, 9 - very pleasant).

	AP	BR	BSG	TS	TM	MS
Appearance	4.83b (SD = 1.64)	6.58a (SD = 1.93)	5.17 ab (SD = 1.7)	5.25 ab (SD = 1.54)	4.25b (SD = 1.29)	4.92b (SD = 2.15)
Texture by touch	4.58a (SD = 1.93)	5.83a (SD = 1.47)	4.83a (SD = 1.7)	5.40a (SD = 2.35)	5.83a (SD = 1.99)	4.83a (SD = 2.44)
Smell	5.58a (SD = 1.08)	6.00a (SD = 1.48)	5.17 ab (SD = 1.19)	5.08a (SD = 1.16)	4.83a (SD = 1.27)	5.42a (SD = 1.83)
Color	5.42 ab (SD = 1.88)	7.17a (SD = 1.85)	5.83 ab (SD = 1.75)	5.50 ab (SD = 1.68)	5.08b (SD = 1.56)	5.17b (SD = 1.7)
Shape	4.17 ab (SD = 1.75)	5.42a (SD = 2.07)	4.75 ab (SD = 1.71)	5.33a (SD = 1.83)	3.33b (SD = 1.56)	5.17 ab (SD = 2.41)
Attractiveness	4.67b (SD = 1.92)	7.00a (SD = 1.35)	5.33 ab (SD = 2.27)	4.92b (SD = 1.88)	4.42b (SD = 1.68)	5.67 ab (SD = 1.83)
Texture in mouth	5.83a (SD = 1.47)	6.08a (SD = 1.16)	5.08a (SD = 1.73)	5.83a (SD = 1.4)	6.25a (SD = 1.6)	6.17a (SD = 1.99)
Layering	5.33a (SD = 1.23)	6.08a (SD = 1.51)	4.83a (SD = 1.9)	5.25 ab (SD = 1.14)	5.58a (SD = 1.31)	5.75a (SD = 1.6)
Taste of the spoon	5.25a (SD = 1.76)	4.92a (SD = 1.93)	4.75a (SD = 2.01)	4.08a (SD = 1.78)	4.33a (SD = 1.3)	3.92a (SD = 1.38)
The smell of the yoghurt on the spoon	5.33a (SD = 0.63)	5.58a (SD = 0.5)	5.00a (SD = 1.36)	4.67a (SD = 1.36)	4.92a (SD = 0.45)	5.08a (SD = 1.53)

Means with different letters are significantly different ($p < 0.05$).

4. Discussion

The introduction outlined the concept of "printability," which refers to the ability of an ink or material to be successfully extruded and maintain structural integrity during 3D food printing. In this context, the key characteristics of the final spoons—look, shape, thickness, and height—were evaluated to understand how rheological properties influence the printability of food inks. Shape and look were rated by panelists, thickness and height were measured. These outcomes were considered in relation to the inks' rheological properties, which determine printability—namely yield stress (τ), elastic recovery (R%), storage modulus (G′), complex viscosity, and tan δ. In summary, all dough formulations exhibited elastic-dominant behaviour ($G' > G''$) and phase angles below 35°, indicating solid-like viscoelasticity favorable for extrusion-based printing. The obtained G′ values (1.3×10^4–3.1×10^4 Pa) were generally higher than the 10^3–10^4 Pa range reported as optimal for cereal-based doughs (Čukelj Mustač et al., 2023). The tan δ values (0.20–0.35) exceeded the 0.14–0.17 window associated with the highest print quality, indicating slightly more viscous behaviour. Among the samples, MS and TM showed the most balanced viscoelastic properties and are expected to provide the best printing performance. AP and BR were the stiffest, requiring higher extrusion pressure for better results, while BSG and TS were more viscous and produced less-defined printed edges.

Dimensional stability of the printed spoons was evaluated by comparing their thickness and height before and after baking. Shape retention (%) was calculated as (dimension after baking/dimension before baking) × 100, where values close to 100 % indicate minimal deformation. Literature on printed cereal doughs considers ≤10 % deviation from the designed dimensions as acceptable for good structural fidelity (L. Zhang et al., 2018). In this study, TS showed the highest retention in thickness (94.9 %) but noticeable height loss (77.7 %), while BSG maintained the greatest overall height (90.8 %). The remaining samples (TM, MS, BR, and AP) exhibited 75–83 % retention in both dimensions, indicating shrinkage typical of baked cereal-based structures but below the acceptable range for post-processed 3D-printed doughs.

Several observable tendencies emerged when comparing spoon characteristics with the rheological behavior of the inks. Spoons made from formulations with higher tan δ values, such as BSG (0.35) and TS (0.31), tended to result in greater spoon thickness (8.27 mm and 9.49 mm, respectively), possibly due to lower structural rigidity allowing more expansion during or after printing. In contrast, inks with higher elastic recovery (R%)—notably BR (35.42 %) and TM (20.09 %)—produced more narrow spoons (7.69 mm and 7.55 mm), suggesting that greater elasticity may limit deformation or enhance post-extrusion shape recovery. Interestingly, the widest spoons were not produced from the most elastic or most viscous inks. For instance, TS, which had the lowest yield stress ($\tau = 277.6$ Pa) and only moderate G′, retained the

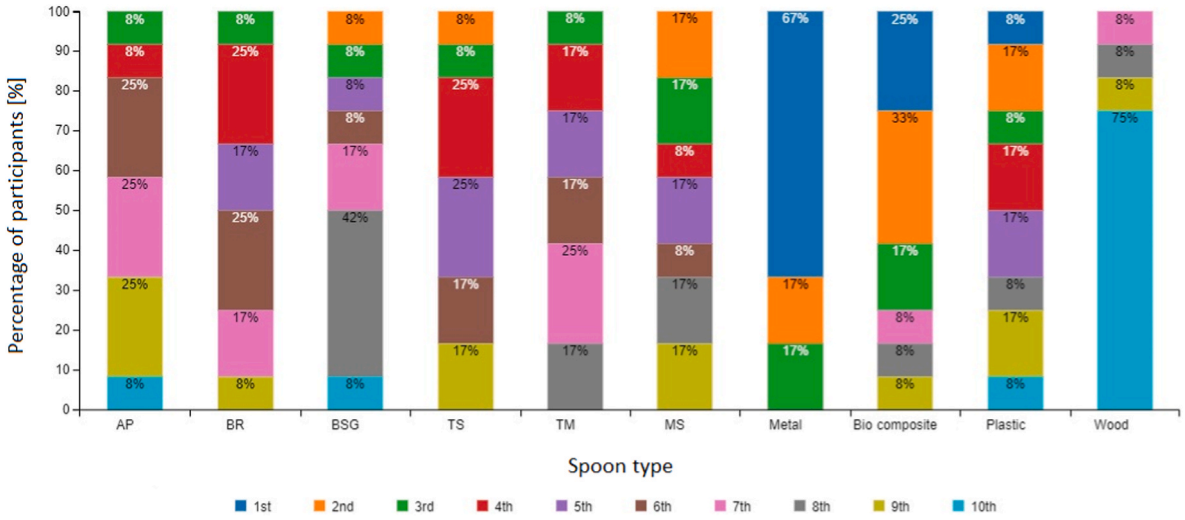

Fig. 4. Ranking distribution of spoon types from most (1st) to least (10th) pleasant to use during food consumption. The chart compares edible spoon prototypes (AP, BR, BSG, TS, TM, MS) to conventional references (metal, biocomposite, plastic, wood). Bars represent the percentage of participants assigning each rank to a given spoon.

greatest thickness, while TM—with the highest G′ (29,121 Pa)—produced one of the thinnest spoons. This suggests that excessive stiffness may inhibit material flow and vertical buildup.

Participants' ratings of shape quality also revealed meaningful trends. TM, despite its highest G′ and intermediate R%, received the lowest shape score (3.33), whereas FR, with high elasticity and yield stress, achieved the highest shape rating (5.42) and was also the most attractive (7.00). MS and TS were also rated highly in shape (5.33 and 5.17), despite having lower G′ values than TM. These findings indicate that excessive stiffness, rather than promoting stability, may reduce both form definition and aesthetic appeal.

Spoons produced from inks with higher tan δ values, such as TS (0.31) and BSG (0.35), were generally well-received in terms of shape (5.17 and 4.75), despite both falling outside the ideal tan δ range of 0.052–0.268 (Gholamipour-Shirazi et al., 2019). This supports the idea that moderate viscoelastic dissipation may be beneficial for shape development, particularly when paired with appropriate yield stress and elasticity levels.

Regarding yield stress, BSG (577.12 Pa) and AP (691.18 Pa) were the only samples falling within the 500–1500 Pa window proposed as optimal for food ink printability (Liu et al., 2020). However, their performance diverged: BSG received a moderate shape rating (4.75), whereas AP scored the lowest (4.17), despite both having similar thickness retention (8.27 mm and 7.66 mm). Conversely, BR—with the highest τ value (2062.4 Pa)—not only printed successfully but was rated highest across most sensory dimensions, including look (6.58), color (7.17), smell (6.00), and attractiveness (7.00). This indicates that high yield stress does not necessarily impede printability if balanced by favorable flow and recovery behavior.

Overall, the results reinforce the understanding that no single rheological parameter can predict printability or user perception. While a high G′ may suggest stability, TM's poor shape and attractiveness scores (3.33 and 4.42) illustrate how excessive rigidity can hinder extrusion and surface quality. Likewise, good print fidelity was observed in samples with tan δ values above the "ideal" range. These findings support earlier claims that emphasized the importance of considering multiple interacting rheological factors—namely elasticity, yield stress, viscoelasticity, and recovery—when evaluating printability and product quality (Kim et al., 2018; Nijdam et al., 2021). The successful extrusion of all samples further indicates that non-Newtonian behavior, shear-thinning, played a critical role in maintaining print continuity and structural definition.

Side streams notably influenced the rheological behavior of the inks in this study. Findings from previous research on doughs enriched with fiber-rich by-products help contextualize these effects. For example, brewer's spent grain (BSG) and apple pomace (AP) increased wheat dough stiffness and storage modulus (G′) due to their high fiber content, while reducing dough extensibility (Ktenioudaki et al., 2013). BSG had a more pronounced effect on increasing the elastic modulus than AP, leading to poorer dough handling. These findings are reflected in this study: both BSG and AP inks showed elevated G′ values, indicating more solid-like behavior. However, AP demonstrated slightly better printability than BSG, consistent with its softer and more deformable structure noted in the literature. Similarly, less refined flours with higher fiber and protein content produced doughs with increased rigidity and elasticity (Iacovino et al., 2024), which is in line with the high G′ values of the BSG and AP inks in our study. Likewise, oat flour increased water absorption but compromised dough stability (Salehifar & Shahedi, 2007), a pattern observed in every ink. Other fiber-rich ingredients, such as grape peel flour (Mironeasa et al., 2019) and onion skin powder (Wang et al., 2025), were shown to enhance dough elasticity and rigidity depending on concentration. In our findings, TS and MS samples achieved good shape integrity and moderate elasticity with mid-range rheological values, suggesting that optimal printability does not depend on elasticity alone, but on a balance between elastic and viscous behavior. On the other hand, despite its high viscosity and structural resistance, the TM ink did not retain shape well. This may be attributed not only to rheological imbalances but also to the composition of the TM residue, which remained somewhat fatty and could have interfered with structural cohesion during and after printing. The side streams used to create inks in this study generally had a negative impact on printability and rheological properties. Additives such as gums or chitosan should be explored as potential enhancers to improve structural integrity and recovery. Other studies support this, showing that extrusion performance and structural integrity can be improved through the addition of functional ingredients like xanthan gum or cellulose nanocrystals (Armstrong et al., 2021; Kim et al., 2018).

Side streams had an effect on the physiochemical properties of the spoons. They demonstrated significantly lower water solubility, ranging between 20 % and 30 %, compared to those made with morning glory powder (Choeybundit et al., 2022). However, these spoons exhibited a much lower swelling rate, from 5 % to 10 %. The spoons also showed water absorption rates of 8 %–12 %, nearly ten times less than those observed in this study. Another study reported even lower water

absorption rates, between 3 % and 13 %, for edible bowls made with BSG flour, finger millet, refined flour, jaggery, and xanthan gum (Nehra et al., 2024). Water absorption rates ranging from 58.50 % to 136.67 % was observed in spoons crafted using mosambi peel and sago powder (Siddiqui et al., 2022). Spoons produced with wheat flour, pearl millet, and barnyard millet exhibited similar water absorption rates varying from 22.05 % to 140.74 % (Rajendran et al., 2020). Oil absorption in bowls ranged from 6 % to nearly 15 % (Nehra et al., 2024), which aligns with the oil absorption rates observed in the spoons analyzed in this research. In 3D-printed bowls 25 % BSG in the formulation improved water resistance (Nehra et al., 2024), but the spoons in this study did not exhibit similar behavior. This could be attributed to β-glucan's high water absorption capacity (Lante et al., 2023) that was not balanced by BSG alone. However, when the other side streams were added spoons still absorbed a lot of water, but did not disintegrate in the same way as a spoon with only BSG.

Brewer's spent grain (BSG) is high in insoluble dietary fiber (38 %) and also contains protein (19 %) and lipids (6 %) on a dry basis (Jin et al., 2022). This mostly insoluble plant material is known to increase G′ and make wheat-based doughs more elastic and less extensible (Amoriello et al., 2020). In our data, the BSG-based ink had relatively high G′ (19 kPa) and a relatively high tan δ (0.35), meaning it behaved as a stiff but still dissipative paste, and it printed with somewhat smeared edges. BSG also showed low recovery after creep (R% = 11.0 %), indicating that once deformed it did not spring fully back; this is consistent with the softer edge definition observed at printing. After baking, BSG spoons kept height very well (90.8 % of the original height), but not thickness (82.7 %). This suggests a drying shrinkage: the insoluble hull/fiber skeleton prevented total vertical collapse, but moisture loss compacted the cross-section.

Similar behavior was observed for sea buckthorn seed side streams. This residue is high in dietary fiber (45 %) and also relatively high in protein (36 %) (data provided by company). That combination should act like a packed particulate–protein composite: it raises elasticity at rest, increases apparent yield stress, and gives the material a way to set under heat. Rheologically, TS ink appeared weak (G′ ≈ 16 kPa, low yield stress 278 Pa) and showed very low elastic recovery after creep (R % = 7.4 %), which would normally predict poorer shape definition immediately after extrusion. However, after baking it held thickness best (94.9 %) and was rated positively for shape. This suggests that TS "self-set" during heating: although it did not recover well under room-temperature shear, its high protein/fiber content likely enabled rapid structural setting in the oven, locking in lateral dimensions. Other two resides showed different behavior. TM originates from sea buckthorn berry pulp/skin material that is relatively low in protein (~3 %), contains moderate sugars (4–5 %) and only modest fibre (6–7 %) (El-Sohaimy et al., 2022). This places it between the high-sugar, pectin-rich pomace formulations (AP, BR) and the high-protein, high--insoluble-fibre press cakes (TS, BSG). MS (blackcurrant seed cake) is closer to the press-cake group: it is very high in dietary fibre (~50 %) but contains less protein (~25 %) than TS (~36 %), and it also retains the highest fat level (~7.5 %). The combination of high fibre (providing structure), lower protein (less rigid protein network than TS), and higher residual fat (plasticising/softening effect) likely prevents MS from behaving either like a highly rigid scaffold (TS, BSG) or like a shrink-prone fruit pomace (AP, BR). As a result, both MS and TM showed mid-range viscoelastic properties (G′ 13.6–17.5 kPa; tan δ 0.25–0.27; recovery 8.6–20.1 %) and mid-range dimensional retention after baking (≈75–76 % thickness; ≈79–82 % height). They did not undergo the strong vertical shrinkage seen in the sugar/pectin-rich pomace systems (AP, BR), nor the axis-specific locking seen in the more fibre/protein-dense formulations (BSG, TS), but instead deformed in a more moderate and symmetric way.

Apple pomace typically contains pectin (10–15 %), insoluble and soluble fiber (up to ~50 % total), and sugars (3–4 %), protein (4 %) and fat (1–4 %) (Valková et al., 2022). Berry pulp is similarly rich in soluble polysaccharides, plus residual sugars after pressing (Jurevičiūtė et al., 2022). These components (pectin, soluble fiber, sugars) bind water and give a cohesive, gel-like dough. That matches what was measured: BR had the highest G′ (30.5 kPa), the highest yield stress (2062 Pa), and the highest recovery (R% = 35.4 %), i.e. it resisted deformation and snapped back after shear. AP was also quite elastic (tan δ = 0.20, phase angle 9.3°) and showed good recovery (25.8 %). These inks held crisp filament definition immediately after deposition. However, after baking, both viaraints lost height substantially (BR: 74.0 % height retained; AP: 82.8 %) and did not keep full thickness (BR: 76.9 %; AP: 76.6 %). This indicates that high elastic recovery at room temperature did not prevent thermal shrinkage. A plausible explanation is that the pectin/sugar-rich matrix contracted as water evaporated and the concentrated network tightened.

All spoon formulations absorbed large amounts of water during 24 h soaking, in most cases close to or above a doubling of their original mass, but they differed in how well they survived that absorption structurally. These differences can be interpreted in terms of the chemical composition of the side streams. BSG is rich in insoluble dietary fibre and also contains a relatively high protein fraction. This combination promotes high water binding and high solubility of carbohydrate material into the soaking medium (Eche et al., 2025), which explains why the BSG spoons disintegrated instead of merely swelling: they took up water, but the hydrated matrix lost cohesion and partially dissolved, consistent with the elevated water solubility and comparatively high oil uptake. When other side streams were used, the behaviour changed. TM, which showed the highest structural resilience after soaking, combined high water absorption with minimal dimensional distortion. This suggests that although TM takes up water into the matrix, it retains an internal network that resists disintegration (Takahashi et al., 2009). MS absorbed somewhat less water overall but showed the largest width swelling; this behaviour is consistent with MS being both highly fibrous and relatively fatty. In MS, the fibre-rich phase can hold water, but the lower protein-to-fat balance compared with sea buckthorn seed material provides less internal reinforcement against lateral spreading, so the spoon relaxes outward rather than breaking apart (Mousia et al., 2007). TS behaved in the same general range of total water uptake as TM and MS — there were no significant differences in overall water absorption between TM, MS, TS, BR, and AP — but it did not undergo the extreme lateral spreading seen in MS or the pronounced vertical swelling seen in AP. TS is derived from defatted sea buckthorn seeds and is rich in both insoluble dietary fibre and protein, with relatively little fat. This composition suggests a dense, protein-reinforced fibre network that absorbs water without dissolving, which explains why TS spoons largely maintained their printed geometry after soaking (Gâtlan & Gutt, 2021; Guyony et al., 2022). AP absorbed the most water overall and showed the greatest increase in thickness, alongside moderately high oil absorption. Apple pomace is low in protein but rich in soluble pectin, which forms highly hydrated gels; this promotes bulk swelling but offers little structural reinforcement once swollen (Schmid et al., 2020), making AP one of the formulations most prone to deformation, together with the BSG spoon. BR also absorbed large amounts of water and, unlike BSG, did not disintegrate or show the pronounced deformation observed in AP. Berry pomace from wine pressing is dominated by insoluble peel/skin fibre, with moderate protein and notable residual fat. That fibrous, skin-derived matrix produced a stiff, shape-holding paste during printing — BR spoons showed the sharpest filament definition and highest elastic recovery — and after hydration it allowed the spoons to soften without fully losing integrity rather than collapsing (Blejan et al., 2023).

5. Limitations and further studies

This study faced several limitations. First, the type of printer used may have influenced the results, as the inks were extruded using air pressure acting on a piston; future work should include printing with a

screw-driven extrusion mechanism. Second, the sensory evaluation was conducted with a limited number of panelists, and a larger cohort is needed to improve the robustness of the results. All inks were printed under identical conditions; however, printing parameters should be optimized separately for each formulation. In addition, further recipe modifications may be necessary for formulations with higher viscosity. Finally, the incorporation of additives that improve water resistance should be considered.

6. Conclusions

This research focused on creating and evaluating 3D-printable edible spoons made from various food production side streams, assessing food ink printability, structural integrity, and user experience. All developed inks exhibited desirable shear-thinning behavior and a dominance of G′ in the linear viscoelastic region. However, their low recovery percentages classified them as viscoelastic liquids. Statistically significant differences in rheological parameters (G′, G″, and yield stress) were observed across formulations, indicating a strong influence of side stream composition on printability. In general, formulations with balanced elasticity, moderate viscosity, and shear-thinning behavior showed better performance in terms of structural retention and consumer acceptability.

Physicochemical tests assessed water and oil absorption, swelling, and solubility. The sea buckthorn berry residue formulation (TM) showed the best structural integrity after soaking, likely due to its high fat content limiting water penetration. In contrast, spoons made solely with brewer's spent grain (BSG) disintegrated in water and had the highest solubility. Coating strategies, such as edible wax layers, may help reduce water uptake and improve functional durability.

Sensory evaluation revealed that the berry pulp-based spoon (BR) was rated highest across most categories, including look, color, smell, and overall attractiveness. The sea buckthorn seed (TS) and blackcurrant seed (MS) formulations also performed well in shape and texture. Edible spoons were generally preferred over wooden and plastic alternatives but were rated lower than metal and biocomposite spoons. In summary, considering both structural performance and sensory appeal, the most promising formulations are those based on berry pulp (BR), sea buckthorn seed (TS), and blackcurrant seed (MS). These should be prioritized for further development and testing in larger-scale consumer studies.

CRediT authorship contribution statement

Marta Stachnik: Writing – original draft, Formal analysis, Data curation, Conceptualization. **Eija Kulju:** Validation, Supervision, Methodology, Conceptualization. **Oskar Laaksonen:** Writing – review & editing, Validation, Supervision, Methodology, Conceptualization.

Use of AI

The authors used AI tools (ChatGPT and Copilot) to improve the grammar, clarity, and style of the manuscript. After using this tool/service, the author reviewed and edited the content as needed and take full responsibility for the content of the published article.

Declaration of competing interest

The authors declare that they have no known competing financial interests or personal relationships that could have appeared to influence the work reported in this paper.

Data availability

Data will be made available on request.

References

Aimar, A., Palermo, A., & Innocenti, B. (2019). The role of 3D printing in medical applications: A state of the art. *Journal of Healthcare Engineering, 2019*, (1), Article 5340616. https://doi.org/10.1155/2019/5340616

Amoriello, T., Mellara, F., Galli, V., Amoriello, M., & Ciccoritti, R. (2020). Technological properties and consumer acceptability of bakery products enriched with brewers' spent grains. *Foods, 9*(10), 1492. https://doi.org/10.3390/foods9101492

Armstrong, A. A., Pfeil, A., Alleyne, A. G., & Wagoner Johnson, A. J. (2021). Process monitoring and control strategies in extrusion-based bioprinting to fabricate spatially graded structures. *Bioprinting, 21*, Article e00126. https://doi.org/10.1016/j.bprint.2020.e00126

Blejan, A. M., Nour, V., Păcularu-Burada, B., & Popescu, S. M. (2023). Wild bilberry, blackcurrant, and blackberry by-products as a source of nutritional and bioactive compounds. *International Journal of Food Properties, 26*(1), 1579–1595. https://doi.org/10.1080/10942912.2023.2224530

Bortolini, D. G., Benvenutti, L., Demiate, I. M., Nogueira, A., Alberti, A., & Zielinski, A. A. F. (2020). A new approach to the use of apple pomace in cider making for the recovery of phenolic compounds. *LWT, 126*, Article 109316. https://doi.org/10.1016/j.lwt.2020.109316

Campos, D. A., Gómez-García, R., Vilas-Boas, A. A., Madureira, A. R., & Pintado, M. M. (2020). Management of fruit industrial by-Products—A case study on circular economy approach. *Molecules, 25*(2). https://doi.org/10.3390/molecules25020320. Article 2.

Caponio, F., Piga, A., & Poiana, M. (2022). Valorization of food processing By-Products. *Foods, 11*(20). https://doi.org/10.3390/foods11203246. Article 20.

Chickering, G., Krause, M. J., & Schwarber, A. (2023). Effects of landfill food waste diversion: A focus on microbial populations and methane generation. *Biodegradation, 34*(5), 477. https://doi.org/10.1007/s10532-023-10034-5

Choeybundit, W., Shiekh, K. A., Rachtanapun, P., & Tongdeesoontorn, W. (2022). Fabrication of edible and biodegradable cutlery from morning glory (*ipomoea aquatic*) stem fiber-reinforced onto soy protein isolate. *Heliyon, 8*(5), Article e09529. https://doi.org/10.1016/j.heliyon.2022.e09529

Costa, J. R., Amorim, M., Vilas-Boas, A., Tonon, R. V., Cabral, L. M. C., Pastrana, L., & Pintado, M. (2019). Impact of in vitro gastrointestinal digestion on the chemical composition, bioactive properties, and cytotoxicity of Vitis vinifera L. cv. syrah grape pomace extract. *Food & Function, 10*(4), 1856–1869. https://doi.org/10.1039/C8FO02534G

Čukelj Mustač, N., Pastor, K., Kojić, J., Voučko, B., Ćurić, D., Rocha, J. M., & Novotni, D. (2023). Quality assessment of 3D-printed cereal-based products. *LWT, 184*, Article 115065. https://doi.org/10.1016/j.lwt.2023.115065

Eche, V., Emenike, C. U., & Rupasinghe, H. P. V. (2025). Nutritional value of brewer's spent grain and consumer acceptance of its value-added food products. *Foods, 14*(16), 2900. https://doi.org/10.3390/foods14162900

El-Sohaimy, S. A., Shehata, M. G., Mathur, A., Darwish, A. G., Abd El-Aziz, N. M., Gauba, P., & Upadhyay, P. (2022). Nutritional evaluation of sea buckthorn "Hippophae rhamnoides" berries and the pharmaceutical potential of the fermented juice. *Fermentation, 8*(8). https://doi.org/10.3390/fermentation8080391. Article 8.

Fahmy, A. R., Amann, L. S., Dunkel, A., Frank, O., Dawid, C., Hofmann, T., Becker, T., & Jekle, M. (2021). Sensory design in food 3D printing – Structuring, texture modulation, taste localization, and thermal stabilization. *Innovative Food Science & Emerging Technologies, 72*, Article 102743. https://doi.org/10.1016/j.ifset.2021.102743

Feng, J., Fu, J., Lin, Z., Shang, C., & Li, B. (2018). A review of the design methods of complex topology structures for 3D printing. *Visual Computing for Industry, Biomedicine, and Art, 1*(1), 5. https://doi.org/10.1186/s42492-018-0004-3

Fernandes, P. C. B., & Silva, J. (2025). Brewing by-products: Source, nature, and handling in the dawn of a circular economy age. *Biomass, 5*(3). https://doi.org/10.3390/biomass5030049. Article 3.

FIT4FOOD2030. (n.d.). FOOD 2030 policy framework. FIT4FOOD2030. Retrieved October 27, 2025, from https://fit4food2030.eu/food-2030/.

Gamero, S., Jiménez-Rosado, M., Romero, A., Bengoechea, C., & Guerrero, A. (2019). Reinforcement of soy protein-based bioplastics through addition of lignocellulose and injection molding processing conditions. *Journal of Polymers and the Environment, 27*(6), 1285–1293. https://doi.org/10.1007/s10924-019-01430-1

Gâtlan, A.-M., & Gutt, G. (2021). Sea buckthorn in plant based diets. An analytical approach of sea buckthorn fruits composition: Nutritional value, applications, and health benefits. *International Journal of Environmental Research and Public Health, 18*(17). https://doi.org/10.3390/ijerph18178986. Article 17.

Gholamipour-Shirazi, A., Norton, I. T., & Mills, T. (2019). Designing hydrocolloid based food-ink formulations for extrusion 3D printing. *Food Hydrocolloids, 95*, 161–167. https://doi.org/10.1016/j.foodhyd.2019.04.011

Godoi, F. C., Prakash, S., & Bhandari, B. R. (2016). 3d printing technologies applied for food design: Status and prospects. *Journal of Food Engineering, 179*, 44–54. https://doi.org/10.1016/j.jfoodeng.2016.01.025

Guyony, V., Fayolle, F., & Jury, V. (2022). Die dimensions impact on fibrous plant protein formation during high moisture extrusion. *Applied Food Research, 2*(2), Article 100228. https://doi.org/10.1016/j.afres.2022.100228

Ha, A. (2023). Bans on plastic straws: Why they happen and where they are. *EQUO*. https://shopequo.com/blogs/blog/plastic-straws-ban.

Hussain, S., Arora, V. K., & Malakar, S. (2021). Formulation of protein-enriched 3D printable food matrix and evaluation of textural, rheological characteristics, and printing stability. *Journal of Food Processing and Preservation, 45*(2). https://doi.org/10.1111/jfpp.15182

Iacovino, S., Trivisonno, M. C., Messia, M. C., Cuomo, F., Lopez, F., & Marconi, E. (2024). Combination of empirical and fundamental rheology for the characterization of

dough from wheat flours with different extraction rate. *Food Hydrocolloids, 148*, Article 109446. https://doi.org/10.1016/j.foodhyd.2023.109446
Jin, Z., Lan, Y., Ohm, J.-B., Gillespie, J., Schwarz, P., & Chen, B. (2022). Physicochemical composition, fermentable sugars, free amino acids, phenolics, and minerals in brewers' spent grains obtained from craft brewing operations. *Journal of Cereal Science, 104*, Article 103413. https://doi.org/10.1016/j.jcs.2022.103413
Jurevičiūtė, I., Keršienė, M., Bašinskienė, L., Leskauskaitė, D., & Jasutienė, I. (2022). Characterization of berry pomace powders as dietary fiber-rich food ingredients with functional properties. *Foods, 11*(5). https://doi.org/10.3390/foods11050716. Article 5.
Kaur, M., Agarwal, C., & Agarwal, R. (2009). Anticancer and cancer chemopreventive potential of grape seed extract and other grape-based products. *The Journal of Nutrition, 139*(9), 1806S–1812S. https://doi.org/10.3945/jn.109.106864
Kim, H. W., Lee, J. H., Park, S. M., Lee, M. H., Lee, I. W., Doh, H. S., & Park, H. J. (2018). Effect of hydrocolloids on rheological properties and printability of vegetable inks for 3D food printing. *Journal of Food Science, 83*(12), 2923–2932. https://doi.org/10.1111/1750-3841.14391
Ktenioudaki, A., O'Shea, N., & Gallagher, E. (2013). Rheological properties of wheat dough supplemented with functional by-products of food processing: Brewer's spent grain and apple pomace. *Journal of Food Engineering, 116*(2), 362–368. https://doi.org/10.1016/j.jfoodeng.2012.12.005
Lante, A., Canazza, E., & Tessari, P. (2023). Beta-glucans of cereals: Functional and technological properties. *Nutrients, 15*(9). https://doi.org/10.3390/nu15092124. Article 9.
Lipton, J., Arnold, D., Nigl, F., Lopez, N., Cohen, D., Norén, N., & Lipson, H. (2010). Multi-material food printing with complex internal structure suitable for conventional post-processing. https://hdl.handle.net/2152/88304.
Liu, Z., Chen, H., Zheng, B., Xie, F., & Chen, L. (2020). Understanding the structure and rheological properties of potato starch induced by hot-extrusion 3D printing. *Food Hydrocolloids, 105*, Article 105812. https://doi.org/10.1016/j.foodhyd.2020.105812
Lugo, S. D. R., Kimita, K., & Nishino, N. (2022). Circular food economy framework: Challenges and initiatives. *Procedia CIRP, 112*, 28–33. https://doi.org/10.1016/j.procir.2022.09.019
Mantihal, S., Prakash, S., Godoi, F. C., & Bhandari, B. (2017). Optimization of chocolate 3D printing by correlating thermal and flow properties with 3D structure modeling. *Innovative Food Science & Emerging Technologies, 44*, 21–29. https://doi.org/10.1016/j.ifset.2017.09.012
Matharu, A. S., de Melo, E. M., & Houghton, J. A. (2016). Opportunity for high value-added chemicals from food supply chain wastes. *Bioresource Technology, 215*, 123–130. https://doi.org/10.1016/j.biortech.2016.03.039
Menard, K. P., & Menard, N. R. (2020). Rheology basic: Creep-recovery and stress relaxation. In *Dynamic mechanical analysis* (3rd ed.). CRC Press.
Mironeasa, S., Iuga, M., Zaharia, D., & Mironeasa, C. (2019). Rheological analysis of wheat flour dough as influenced by grape peels of different particle sizes and addition levels. *Food and Bioprocess Technology, 12*(2), 228–245. https://doi.org/10.1007/s11947-018-2202-6
Mousia, Z., Campbell, G. M., Pandiella, S. S., & Webb, C. (2007). Effect of fat level, mixing pressure and temperature on dough expansion capacity during proving. *Journal of Cereal Science, 46*(2), 139–147. https://doi.org/10.1016/j.jcs.2006.12.006
Mussatto, S. I., & Roberto, I. C. (2008). Establishment of the optimum initial xylose concentration and nutritional supplementation of brewer's spent grain hydrolysate for Xylitol production by *Candida guilliermondii*. *Process Biochemistry, 43*(5), 540–546. https://doi.org/10.1016/j.procbio.2008.01.013
Natarajan, N., Vasudevan, M., Vivekk Velusamy, V., & Selvaraj, M. (2019). Eco-friendly and edible waste cutlery for sustainable environment. *International Journal of Engineering and Advanced Technology, 9*(1S4). https://doi.org/10.35940/ijeat.A1031.1291S419
Nehra, A., Biswas, D., & Roy, S. (2024). Fabrication of brewer's spent grain fortified bio-based edible bowls: A promising alternative to plastic containers. *Biomass Conversion and Biorefinery, 14*(14), 16425–16434. https://doi.org/10.1007/s13399-022-03698-1
Nijdam, J. J., Agarwal, D., & Schon, B. S. (2021). Assessment of a novel window of dimensional stability for screening food inks for 3D printing. *Journal of Food Engineering, 292*, Article 110349. https://doi.org/10.1016/j.jfoodeng.2020.110349
Oh, Y., Lee, S., Lee, N. K., & Rhee, J.-K. (2024). Improving the three-dimensional printability of potato starch loaded onto food ink. *Journal of Microbiology and Biotechnology, 34*(4), 891. https://doi.org/10.4014/jmb.2311.11040
Olajire, A. A. (2020). The brewing industry and environmental challenges. *Journal of Cleaner Production, 256*, Article 102817. https://doi.org/10.1016/j.jclepro.2012.03.003
Osei, E. D., Naik, A. S., Kinsella, G., Delaney, T., & Kirwan, S. (2025). Potential of Brewer's spent grain bioactive fractions as functional ingredients for companion and farm animal foods – A review. *Applied Food Research, 5*(2), Article 101138. https://doi.org/10.1016/j.afres.2025.101138
Oztuna Taner, O., Ekici, L., & Akyuz, L. (2023). CMC-based edible coating composite films from Brewer's spent grain waste: A novel approach for the fresh strawberry package. *Polymer Bulletin, 80*(8), 9033–9058. https://doi.org/10.1007/s00289-022-04490-x
Park, S., Shou, W., Makatura, L., Matusik, W., & Fu, K. K. (2022). 3D printing of polymer composites: Materials, processes, and applications. *Matter, 5*(1), 43–76. https://doi.org/10.1016/j.matt.2021.10.018
Paudel, D., Dhungana, B., Caffe, M., & Krishnan, P. (2021). A review of health-beneficial properties of oats. *Foods, 10*(11), 2591. https://doi.org/10.3390/foods10112591
Pulatsu, E., & Lin, M. (2021). A review on customizing edible food materials into 3D printable inks: Approaches and strategies. *Trends in Food Science & Technology, 107*, 68–77. https://doi.org/10.1016/j.tifs.2020.11.023
Rajendran, S. P., Saravanan, A., Namachivayam, G. K., Jambunathan, J., & Ramachandran, G. (2020). Optimization of composition for preparation of edible cutlery using response surface methodology (RSM). In *AIP conference proceedings* (Vol.2240)AIP Publishing. 3RD NATIONAL CONFERENCE ON CURRENT AND EMERGING PROCESS TECHNOLOGIES – CONCEPT 2020. https://doi.org/10.1063/5.0011042, 1.
Rishi, P., Zade, T., Abhiraj, P., Pandey, V. S., & Roy, S. (2024). Exploring the potential of ragi, wheat, and rice flours as a sustainable solution for edible bowl: A suitable substitution for disposable plastic bowl. *Food and Humanity, 3*, Article 100455. https://doi.org/10.1016/j.foohum.2024.100455
Roy, R. T., & Morya, S. (2022). Edible cutlery: An eco-friendly replacement for plastic cutlery | journal of applied and natural science. *Journal of Applied and Natural Science, 14*(3), 835–843. https://doi.org/10.31018/jans.v14i3.3627
Salehifar, M., & Shahedi, M. (2007). Effects of oat flour on dough rheology, texture and organoleptic properties of taftoon bread. *Journal of Agricultural Science and Technology A, 9*(3), 227–234.
Schmid, V., Trabert, A., Schäfer, J., Bunzel, M., Karbstein, H. P., & Emin, M. A. (2020). Modification of apple pomace by extrusion processing: Studies on the composition, polymer structures, and functional properties. *Foods, 9*(10), 1385. https://doi.org/10.3390/foods9101385
Shroti, G. K., & Saini, C. S. (2022). Development of edible films from protein of brewer's spent grain: Effect of pH and protein concentration on physical, mechanical and barrier properties of films. *Applied Food Research, 2*(1), Article 100043. https://doi.org/10.1016/j.afres.2022.100043
Siddiqui, S. A., Zannou, O., Karim, I., Kasmiati, Awad, N. M. H., Gołaszewski, J., Heinz, V., & Smetana, S. (2022). Avoiding food neophobia and increasing consumer acceptance of new food trends—A decade of research. *Sustainability, 14*(16), Article 10391. https://doi.org/10.3390/su141610391
Singh, R. S., & Saini, G. K. (2012). Biosynthesis of pullulan and its applications in food and pharmaceutical industry. In T. Satyanarayana, & B. N. Johri (Eds.), *Microorganisms in sustainable agriculture and biotechnology* (pp. 509–553). Netherlands: Springer. https://doi.org/10.1007/978-94-007-2214-9_24.
Takahashi, T., Furuichi, Y., Mizuno, T., Kato, M., Tabara, A., Kawada, Y., Hirano, Y., Kubo, K., Onozuka, M., & Kurita, O. (2009). Water-holding capacity of insoluble fibre decreases free water and elevates digesta viscosity in the rat. *Journal of the Science of Food and Agriculture, 89*(2), 245–250. https://doi.org/10.1002/jsfa.3433
Tarancón, P., Hernández, M. J., Salvador, A., & Sanz, T. (2015). Relevance of creep and oscillatory tests for understanding how cellulose emulsions function as fat replacers in biscuits. *LWT - Food Science and Technology, 62*(1), 640–646. https://doi.org/10.1016/j.lwt.2014.06.029, 2.
Thai, S., Avena-Bustillos, R. J., Alves, P., Pan, J., Osorio-Ruiz, A., Miller, J., Tam, C., Rolston, M. R., Teran-Cabanillas, E., Yokoyama, W. H., & McHugh, T. H. (2022). Influence of drying methods on health indicators of brewers spent grain for potential upcycling into food products. *Applied Food Research, 2*(1), Article 100052. https://doi.org/10.1016/j.afres.2022.100052
Valková, V., Ďúranová, H., Havrlentová, M., Ivanišová, E., Mezey, J., Tóthová, Z., Gabríny, L., & Kačániová, M. (2022). Selected physico-chemical, nutritional, antioxidant and sensory properties of wheat bread supplemented with apple pomace powder as a By-Product from juice production. *Plants, 11*(9). https://doi.org/10.3390/plants11091256. Article 9.
Yavagal, P. S., Kulkarni, P. A., Patil, N. M., Salimath, N. S., Patil, A. Y., Savadi, R. S., & Kottursettar, B. B. (2020). Cleaner production of edible straw as replacement for thermoset plastic. *Materials Today: Proceedings, 32*, 492–497. https://doi.org/10.1016/j.matpr.2020.02.667
Zhang, L., Lou, Y., & Schutyser, M. A. I. (2018). 3D printing of cereal-based food structures containing probiotics. *Food Structure, 18*, 14–22. https://doi.org/10.1016/j.foostr.2018.10.002
Zhang, J.-P., Ma, L.-C., Ruan, Y.-J., Lu, Y.-Y., & An, L.-J. (2024). Evolution of polymer melt conformation and entanglement under high-rate elongational flow. *Chinese Journal of Polymer Science, 42*(12), 2021–2029. https://doi.org/10.1007/s10118-024-3170-0